Journal of Engineering and Applied Sciences 11 (10): 2146-2154, 2016
ISSN: 1816-949X

Simplified Approach to Validate Constitutive Model Formulation of Orthotropic Materials Undergoing Finite Strain Deformation

Mohd Khir Mohd Nor and Norzarina Ma'at
Crashworthiness and Collisions Research Group,
Faculty of Mechanical Engineering and Manufacturing,
Universiti Tun Hussein Onn Malaysia, Beg Berkunci 101 Parit Raja,
Batu Pahat, 86400 Johor, Malaysia

Abstract: Modelling finite strain deformation including shockwave propagation in orthotropic materials requires an appropriate description of material behaviour within elastic and plastic regimes hence can be very complex. One of the real challenges of this research is to accurately validate each of the proposed formulation since the corresponding algorithm implementation normally involves more than thousand lines of code. The validation process must be systematically conducted by stages from simple to complex behaviours. In this study, a new approach was developed and established to guide through this processes by referring to the newly constitutive model formulation applicable for finite strain deformation. The chosen constitutive model was implemented into the DYNA3D source code. The validation process was performed by conducting a series of a single element analysis of a uniaxial strain test and uniaxial stress test. The formulations of elastic isotropy, elastic orthotropy and elastic-plastic isotropy orthotropy (with and without hardening) of the proposed formulation were examined and validated against DYNA3D Material Types 10, 22 and 33, respectively in this stage. To really ensure the book-keeping of the proposed algorithm is clean and efficient the analysis on multiple elements analysis was performed. For this purpose, a plate impact test has been adopted on the elastic isotropy and elastic orthotropy analyses. The capability of the proposed formulation to capture the dependence of material under consideration on strain rate and temperature was finally investigated. A good agreement with respect to various flow stress conditions was obtained. The results then established the capability of the proposed formulation and its algorithm implementation before validation against the selected experimental tests can be conducted.

Key words: Finite strain deformation, shockwave propagation, orthotropic materials, single element analysis, multiple element analysis, DYNA3D

INTRODUCTION

In practice, in the real world, most of the engineering materials such as composites and sheet metal components, manufactured using sheet metal forming processes, are orthotropic. Sheet forms of aluminium alloy are examples of orthotropic materials. Furthermore, many engineering materials such as fibre-reinforced elastomers or glassy polymers exhibit orthotropic behaviour while undergoing large elasto-plastic deformation. The constitutive models intended to represent plastic behaviour are of great importance in the current design and analysis of forming processes due to their broad engineering application (Mohd *et al*., 2013).

The development of constitutive formulation of such materials is very complex due to the mechanics of plastic behaviour. It can be observed that the theory related to isotropic materials is not very complex. It may therefore undergo rotations without affecting the material response. However, this is not the case for orthotropic materials hence reflect to the corresponding algorithm development in the implementation work. The generated algorithm is important and must be systematically validated to ensure an appropriate prediction with respect to the structural components behaviours; the elastic behaviour, hardening, rate dependency and thermal softening.

The purpose of this study, therefore is to present a simplified approach to validate the constitutive model for orthotropic materials that is capable of dealing with material orthotropy (in both elastic and plastic regimes), isotropic hardening, strain rate and temperature effects.

Corresponding Author: Mohd Khir Mohd Nor, Crashworthiness and Collisions Research Group,
Faculty of Mechanical Engineering and Manufacturing, Universiti Tun Hussein Onn Malaysia,
Beg Berkunci 101 Parit Raja, Batu Pahat, 86400 Johor, Malaysia

A newly constitutive model proposed for orthotropic materials undergoing finite strain deformations was used to demonstrate this research (Mohd *et al*., 2013; Mohd, 2016). The proposed validation approach can be adopted to validate other related constitutive models regardless of the chosen simulation tools. The important features of this constitutive model are the multiplicative decomposition of the deformation gradient and a new Mandel stress tensor combined with the new stress tensor decomposition. The elastic free energy function and the yield function are defined within an invariant theory by means of the introduction of the evolving structural tensors used to describe the material symmetry. The plastic orthotropy is characterised by the Hill's yield criterion. The thermally micromechanical-based model, Mechanical Threshold Model (MTS) is adopted as a referential curve to control the yield surface expansion that accounts for isotropic plastic hardening. This constitutive model is developed and integrated in the isoclinic intermediate configuration. The proposed constitutive model was implemented into the DYNA3D source code, named as Material Type 93 (mat93).

MATERIALS AND METHODS

Validation framework: The proposed validation framework is to deeply examine and validate each part of the proposed formulation and its implementation DYNA3D source code, i.e., the validation of elastic isotropic behaviour, the validation of orthotropic elastic behaviour and the validation of orthotropic elastic-plastic behaviour which include strain rate and temperature sensitivity tests. A schematic representation of the whole validation process is given in Fig. 1. The study focuses on this simplified validation process.

The next stage of the validation process is a comparison of the results generated by the proposed constitutive model against the available experimental data from a plate impact and taylor cylinder impact tests. The results of this validation part are omitted in this study however can be found in the other publications to show the effectiveness of the simplified approach used in the first validation part (Mohd *et al*., 2013; Mohd, 2016). A units system was adopted in the involved numerical tests.

Finite element model for uniaxial stress and uniaxial strain tests: In order to validate the model for the uniaxial strain and uniaxial stress states, a series of one element analysis were performed. The single element with the node numbering used to define boundary conditions is shown in Fig. 2.

In this model the principle directions of material orthotropy were aligned with the x, y, z axis of the global coordinate system. For brevity, only the tests performed in x direction are presented and discussed. The displacement boundary conditions applied in these tests are summarised in Table 1. Loading in compression and tension was applied to the elements by prescribing displacement load curves to nodes 1-4. The equivalent tests were performed for the y and z directions. In order to speed up the comparison process, two solid elements with identical geometry, boundary conditions and loading were used in each simulation as shown in Fig. 3.

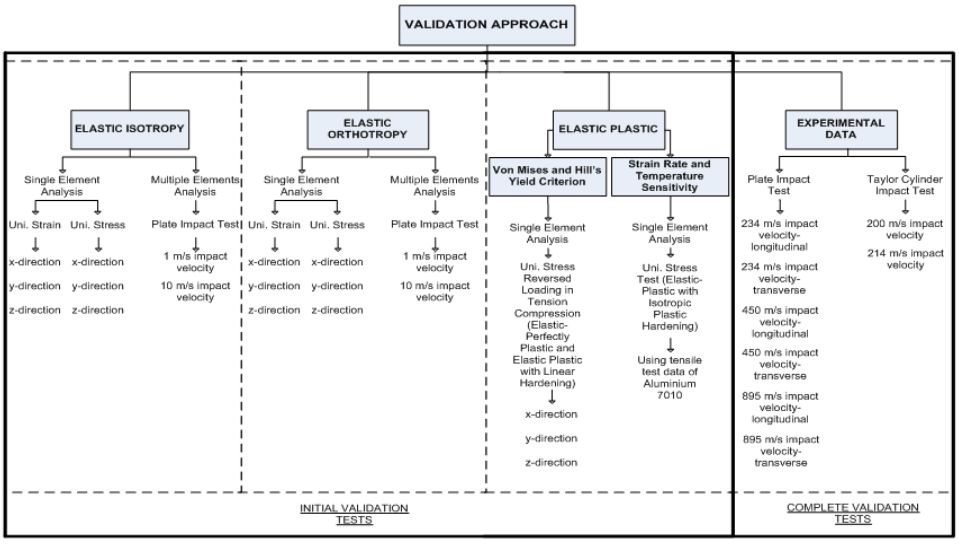

Fig. 1: Schematic representation of the proposed approach

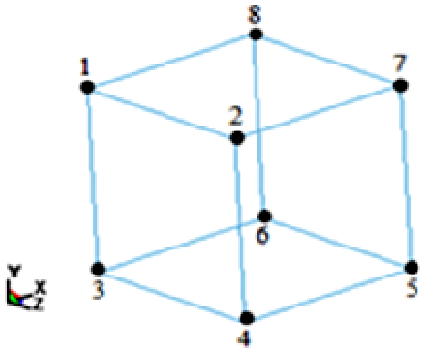

Fig. 2: Single element configuration

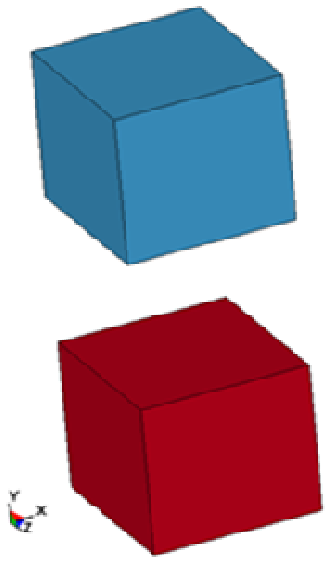

Fig. 3: The finite element model used in the single element analysis

Table 1: Displacements boundary conditions for a uniaxial stress and uniaxial strain tests in the x direction

Displacement boundary condition	
Uniaxial stress	Uniaxial strain
No constraints	Constrained y and z displacements
No constraints	Constrained y and z displacements
No constraints	Constrained y and z displacements
No constraints	Constrained y and z displacements
Constrained x, y and z displacements	Constrained x, y and z displacements
Constrained x displacement	Constrained x, y and z displacements
Constrained x displacement	Constrained x, y and z displacements
Constrained x displacement	Constrained x, y and z displacements

In this model one element was assigned the new material model and the other a reference material model available in DYNA3D. This allowed for effective comparison of the new material model against the reference material models.

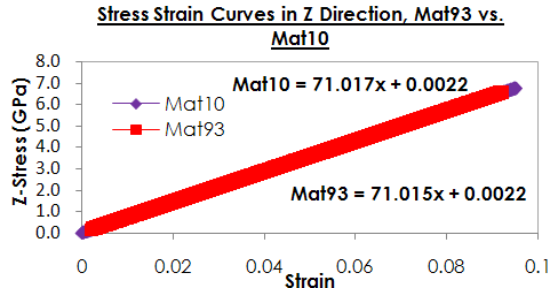

Fig. 4: Stress strain curves comparison between material type 93 and 10 in z direction of uniaxial stress

Table 2: Aluminium material properties for elastic isotropy analysis

Young's modulus	Poisson's ratio	Shear modulus	Bulk modulus
71.00 GPa	0.30	26.75 GPa	69.75 GPa

Validation of elastic isotropy formulation: The first test was intended to make sure the implemented material model is capable of reproducing isotropic behaviour using a series of one element analyses of the uniaxial strain and uniaxial stress states. For this purpose Material Type 10 (Isotropic-Elastic-Plastic-Hydrodynamic) was used as a reference for comparison (Lin, 2004).

The reference material model was given the same elastic properties and a high value of yield in order to prevent the material from yielding for the range of deformations applied. The elastic material properties used in this analysis are given in Table 2. The density of aluminium that was used throughout the validation process is 2.81 g cm^{-3}. The elastic isotropy formulation of the new material model was first validated in this work. At this stage, the trial value of the new deviatoric Mandel stress tensor had to be examined. Therefore, the plasticity and hardening formulations related to the Hill's yield criterion were avoided.

Uniaxial stress results for elastic isotropy: Using the uniaxial stress data, the true stress vs. true strain curves for the x, y, z direction tests were plotted for both material models. The value of Young's modulus calculated from the slopes of the stress strain curves was the same as the value in the input file. For brevity, only the result performed in z direction is presented as shown in Fig. 4. It is obvious that the stress strain curves for both the new and the reference material were identical. This is the simplest part that involves few lines of code however very important for the start of the implementation work. It can be concluded that the newly constitutive model is appropriate of reproducing uniaxial stress states of elastically isotropic materials. The same results were obtained in x and y directions.

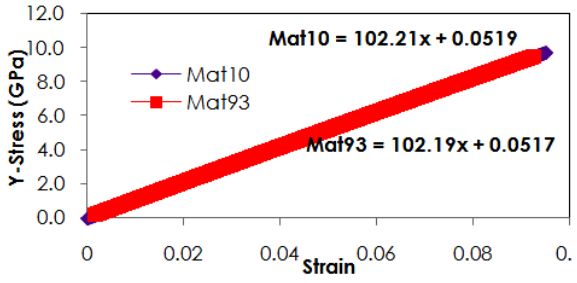

Fig. 5: Stress strain curves comparison between material type 93 and 10 in y direction of uniaxial strain

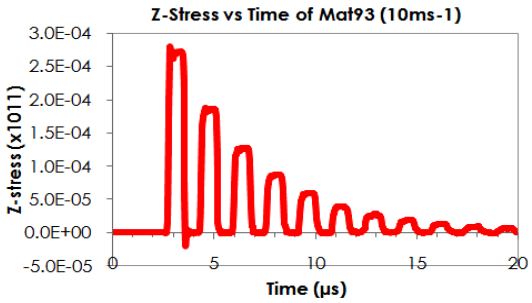

Fig. 6: Longitudinal z-stress of material type 93 at m sec^{-1} impact velocity (elastic isotropy)

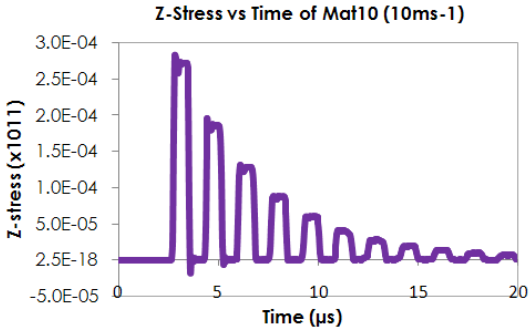

Fig. 7: Longitudinal z-stress of material type 10 at 10 m sec^{-1} impact velocity (elastic isotropy)

Uniaxial strain results for elastic isotropy: In the uniaxial strain state, the material is subjected to axial stress and pressure that develop an axial strain without strain in the radial direction. The confining pressure is increased to force the radial strain back to zero in the case of the radial strain starting to increase (Thomas *et al*., 2008). In addition, the constraints applied in the uniaxial strain test generally can avoid the stress state of the material from reaching the strength limit. Therefore, failure is prevented. By using a single element analysis for the uniaxial strain test, the validation of the implemented deformation gradient in the newly constitutive model is greatly simplified. Equally, this analysis indirectly validates the formulations related to the deformation gradient.

In this research, the uniaxial strain data was analysed by plotting the true stress vs. true strain curves of material type 10 and the new material for the x, y, z directions. The value for the material stiffness in each direction, calculated from the slopes of these curves was equal to K+4G/3 where K is bulk modulus again, for brevity only single direction used to show the results as shown in Fig. 5. It is obvious that the stress strain curves for both the new and the reference material were identical in the chosen y direction.

Therefore, it can be concluded that the new constitutive model is appropriate of reproducing uniaxial strain states of elastically isotropic materials. Furthermore, the implementation of the deformation gradient tensor is also validated.

To ensure an efficient book keeping, the algorithm developed in the implementation process was first accessed by performing multiple elements. The plate impact test was used for this purpose where a good agreement was obtained as shown in Fig. 6 and 7 (Mohd, 2012). Referring to these figures, it can be observed that the longitudinal stress (Z stress) of both material models is virtually identical in every aspect and captures the correct behaviour of material elasticity.

Strictly speaking, no plastic slope was generated as the Hugoniot stress curve was developed immediately after the increment of elastic curve (due to elastic loading). Therefore, no Hugoniot Elastic Limit slope HEL can be observed. Accordingly, the part of the unloading curve (after the Hugoniot stress curve) also showed no plastic unloading. This is due to the low impact velocities applied on the specimen (10 m sec^{-1}).

Based on the results obtained from a single element and multiple elements analyses, it can be deduced that the proposed constitutive model is appropriate of capturing the elastic behaviour of isotropic materials. Furthermore, this had also ensured an efficient algorithm was proposed.

Validation of elastic orthotropy formulation: The elastic orthotropic part of the new constitutive model was first assessed in the single element tests. The same two element model, described previously, was used but this time with the elastically orthotropic material (Mohd, 2012). Therefore, the new material was expected to provide the correct values of Young's modules (as determined by material type 22 Fiber Composite with Damage) for different material directions (AOPT). There are several material axes definitions used in the DYNA3D code;

Table 3: Comparison results of elastic orthotropy in uniaxial stress analyses

Tested directions/AOPT 2	Young's modulus	
	Material type 22	Material type 93
x-direction		
$a = 0a_x+0a_y+1a_z$, $d = 0d_x+1d_y+0d_z$	70.60 GPa	70.60 GPa
$a = 0a_x+1a_y+0a_z$, $d = -1d_x+0d_y+0d_z$	71.10 GPa	71.17 GPa
$a = 0a_x+1a_y+0a_z$, $d = 1d_x+0d_y+0d_z$	71.10 GPa	71.10 GPa
y-direction		
$a = 0a_x+0a_y+1a_z$, $d = 0d_x+1d_y+0d_z$	71.10 GPa	71.17 GPa
$a = 0a_x+1a_y+0a_z$, $d = 1d_x+0d_y+0d_z$	70.60 GPa	70.60 GPa
$a = 1a_x+0a_y+0a_z$, $d = 0d_x+1d_y+0d_z$	71.10 GPa	71.17 GPa
z-direction		
$a = 0a_x+0a_y+1a_z$, $d = 0d_x+1d_y+0d_z$	70.60 GPa	70.59 GPa
$a = 0a_x+1a_y+0a_z$, $d = 1d_x+0d_y+0d_z$	70.60 GPa	70.59 GPa
$a = 1a_x+0a_y+0a_z$, $d = 0d_x+1d_y+0d_z$	70.60 GPa	70.59 GPa

Table 4: Comparison results of elastic orthotropy in uniaxial stress analyses

Tested directions/ orientation of AOPT 2	Young's modulus	
	Material type 22	Material type 93
x-direction		
$a = 0a_x+0a_y+1a_z$, $d = -1d_x+0d_y+0d_z$	110.32 GPa	110.32 GPa
$a = 0a_x+0a_y+1a_z$, $d = 0d_x+1d_y+0d_z$	109.65 GPa	109.65 GPa
$a = 1a_x+0a_y+0a_z$, $d = 0d_x+0d_y-1d_z$	109.44 GPa	109.43 GPa
y-direction		
$a = 0a_x+1a_y+0a_z$, $d = -1d_x+0d_y+0d_z$	109.44 GPa	109.43 GPa
$a = 0a_x+1a_y+0a_z$, $d = 1d_x+0d_y+0d_z$	109.44 GPa	109.43 GPa
$a = 0a_x+0a_y+1a_z$, $d = 0d_x+1d_y+0d_z$	110.32 GPa	110.32 GPa
z-direction		
$a = 1a_x+0a_y+0a_z$, $d = 0d_x+0d_y-1d_z$	110.32 GPa	110.32 GPa
$a = 1a_x+0a_y+0a_z$, $d = 0d_x+1d_y+0d_z$	109.65 GPa	109.65 GPa
$a = 0a_x+0a_y+1a_z$, $d = 0d_x+1d_y+0d_z$	109.44 GPa	109.43 GPa

however, only material axes type 2 (globally orthotropic) was considered in this analysis, In the DYNA3D code, the user is required to define the x, y and z components of vectors a and d in the input file:

$$a = a_x + a_y + a_z; b = d = d_x + d_y + d_z \quad (1)$$

For instance, if the vectors are defined as $a = 0a_x+0a_y+0a_z$ and $d = 0d_x+0d_y+0d_z$ then we get the following vectors' orientation representing the orthotropic material axes of the orthotropic material model:

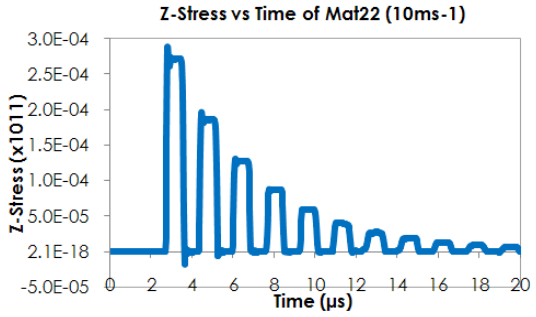

Fig. 8: Longitudinal z-stress of material type 22 at 10 m sec^{-1} impact velocity (elastic orthotropy)

$$\begin{aligned} a &= 0a_x + 0a_y + 1a_z \ z-\text{axis of DYNA} \\ b &= d = 0d_x + 1d_y + 0d_z \ y-\text{axis of DYNA} \\ c &= 1c_x + 0c_y + 0c_z \ x-\text{axis of DYNA} \end{aligned} \quad (2)$$

Uniaxial stress results for elastic orthotropy: Bor brevity, the elastically orthotropic material properties determined from the numerical stress strain curves are summarized in Table 3. It can be clearly observed that the values obtained for the new constitutive model agree well with the values obtained for the reference material model material type 22.

Uniaxial strain analysis of elastic orthotropy formulation: The uniaxial strain analysis performed on the two element model further validated the elastic orthotropic part of the new constitutive model . The results of these analyses are given in Table 4. It is obvious that the stress strain curves for both the new and the reference material were identical.

The capability of the new material model algorithm to provide a clean and efficient book keeping was further examined by checking the elastic orthotropy formulation with multiple elements analysis. A plate impact test again was adopted in these analyses. It can be observed from Fig. 8 and 9 that the longitudinal stress (z-stress) of both material types 22 and 93 are identical. No plastic slope was developed during the loading-unloading part of these curves which were ultimately due to low impact velocities (10 m sec^{-1}). Therefore, no Hugionot Elastic Limit (HEL) can be determined from this material.

Referring to the analyses performed in this stage, it can be clearly seen that the elastic orthotropy formulation was correct while a clean and efficient book keeping was also validated.

Validation of the elastic-plastic formulation: In this part of the validation process, the plasticity part of the new

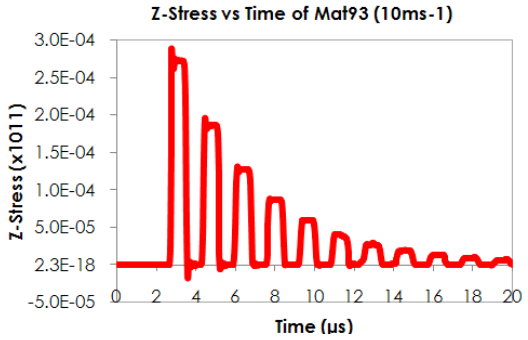

Fig. 9: Longitudinal z-stress of material type 93 at 10 m sec^{-1} impact velocity (elastic orthotropy)

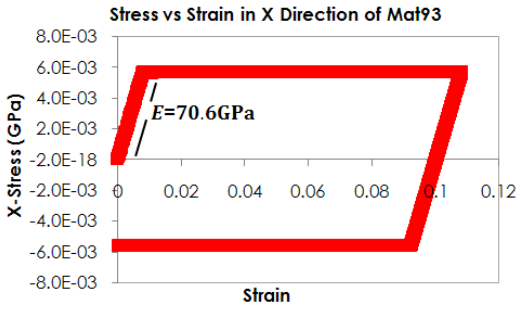

Fig. 10: Stress vs. strain curve, reversed loading elastic perfectly plastic of uniaxial stress test in x direction

constitutive model can be assessed. The first set of tests included validation of Hill's yield criterion for the isotropic elastic-perfectly plastic material. The second set of tests covered the orthotropic elastic-plastic material with linear hardening, while the orthotropic elastic-plastic material with isotropic plastic hardening was examined in the final part of this validation stage.

The first and third sets of tests were performed with aluminium material properties while the second set was performed with tantalum material properties (material with more pronounced anisotropy). All of these tests were performed based on the single element uniaxial stress analysis as described in the previous subsections and adopted a few modifications. Strictly speaking, the prescribed displacement load curve was defined so that the material is first brought to yield in tension and then the loading was reversed to force the material to yield in compression (the reversed loading tests). From the results, it can be concluded that the elastic behaviour of orthotropic materials produced by the implemented algorithm of material type 93 is validated.

Single element analysis of the elastic-perfectly plastic model: In this uniaxial reversed loading test a single element was loaded in tension and compression in x, y, z directions. The material orthotropic properties were set to the isotropic case, i.e., given the same values. In this analysis the tests with an isotropic yield surface, Hill's coefficients were given values as follows, F= G =H = 0.5 and L = M = N = 1.5 in order to reduce the Hill's yield criterion to the von Mises yield criterion. To be precise, Hill's parameters had to be converted into Langford parameters R, P, Q_{bc}, Q_{ba}, Q_{ca}, i.e., the input parameters required by DYNA3D.

The performance of the model was assessed by evaluating the yield stress and the Young's modulus from the output stress strain curves for each direction and in each tension and compression. The example result of this analysis in x direction is shown in Fig. 10. The identical behaviour captured in the other directions

It can be observed that the new constitutive model can appropriately capture the behaviour of the elastic-plastic isotropy of materials (von Mises yield surface) since the yield stress for the x, y, z directions had the same (within the bounds of numerical round off) values for the three directions. The identical yield stress in both tension and compression was expected to be obtained from the new material model due to no Bauschinger effect considered in the proposed formulation

Single element analysis of the elastic-plastic model with linear hardening: The next stage of the proposed validation process of the new orthotropic model was to show that this constitutive model is capable of describing the elastic-plastic with hardening behaviour of metals. To simplify the analysis, the results generated by the new constitutive model were compared directly with the results produced by the material type 33 (General Anisotropic Elastic-Plastic). Again, the specific values of the material properties (tantalum-pronounced orthotropic materials) used can be found in Mohd (2012). The density of tantalum was set to 16.64 g cm^{-3}. Accordingly, the tangent plastic modulus was used to define the hardening part. At this stage, almost all formulations of the new constitutive model except the plastic hardening law load curve (the MTS model) were undergoing validation.

The reversed loading single element tests used in the previous analysis were repeated but this time on a hardening material. The identical behaviour in tension and compression was expected from both material models in this analysis. By setting the material axes AOPT 2 to $a = 0a_x+0a_y+1a_z$ and $d = 0d_x+1d_y+0d_z$, the result obtained in y direction is presented in Fig. 11. The identical responses were obtained in x and z directions.

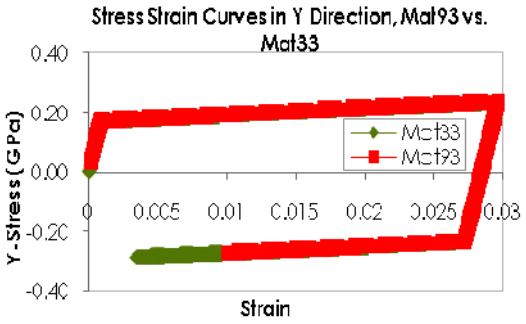

Fig. 11: Stress vs. strain curve, reversed loading elastic-plastic with hardening of uniaxial stress test in y direction

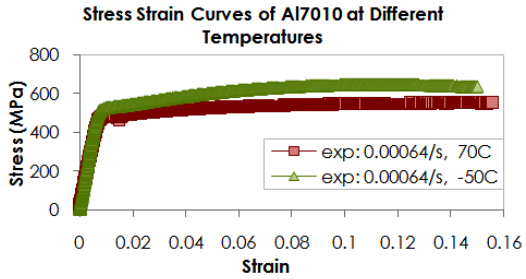

Fig. 12: Stress strain curves of aluminium 7010 at 6.4×10^{-4}/sec at different temperatures direction

Referring to Fig. 11, it can be observed that Material Type 93 has successfully captured the elastic-plastic with hardening behaviours of Tantalum. The identical curves were provided by both material models within elastic-plastic regimes in x and z directions. The Young's modulus, yield stress and the hardening slopes were identical in tension and compression and perfectly matched the given material properties.

Single element analysis of the elastic-plastic model with isotropic plastic hardening: The final stage of the single element analysis approach was conducted to investigate rate sensitivity and temperature sensitivity of the new constitutive model by examining the elastic-plastic model with isotropic plastic hardening of the proposed constitutive model. The tensile test data of Aluminium 7010 published by Panov (2006) was used in this validation stage. The stress-strain curves for quasi-static tension tests (6.4×10^{-4}/sec strain rate) conducted at -50° and 70°C are presented in Fig. 12. In addition, Fig. 13 shows the stress-strain curves of the specimen tested at 140°C at two different strain rates; 6.4×10^{0}/sec and 6.4×10^{1}/sec. It can be clearly seen from these figures that the specimen exhibits strain rate and temperature sensitivity. Referring to Fig. 14, point D refers to the ultimate tensile strength UTS which occurs at maximum

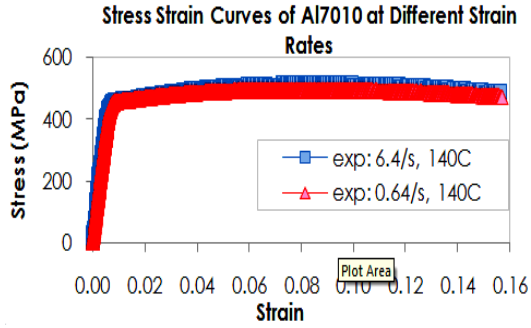

Fig. 13: Stress strain curves of Aluminium 7010 at 140°C at different strain rates

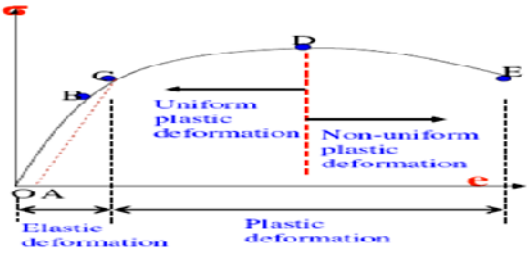

Fig. 14: Materials deformation curve

load while point E refers to the fracture or failure of the tensile test specimen. From yield point C to UTS point D, the plastic deformation represented by the changes of the specimen length is uniform and homogeneous. At point D, the tensile stability is no longer sustainable hence necking or localised deformation starts to develop.

After this point, the plastic deformation in the specimen is concentrated in the small necked area and finally ended up with the specimen failure. Basis on the this discussion, it is important to be aware that any constitutive model that formulated without damage and failure models will be very difficult to track the plastic deformation after the UTS point D.

Therefore, the comparison between the proposed constitutive model and the tensile test data is fairly valid until point D before the plastic deformation occurs non-uniformly in the test specimen. Therefore, the validation process was simplified by using a single element uniaxial stress analysis, as described previously, as the specimen is stretched uniformly without localisation or necking.

Strictly speaking, there was no requirement to simulate the whole event of the tensile test with the real flat dog bone specimen to capture the materials flow stress up to point D. Assuming the single element represents one of the elements around the gauge length, the uniform plastic deformation (from points C to D) is observable using this simplified analysis. The results of this analysis are shown in Fig. 15-18

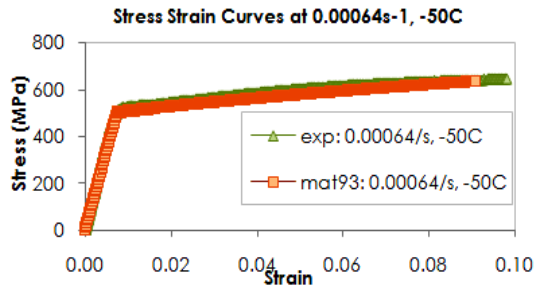

Fig. 15: Stress strain curves comparison between Mat93 and experimental data at 6.4×10^{-4} sec^{-1}, -50°C

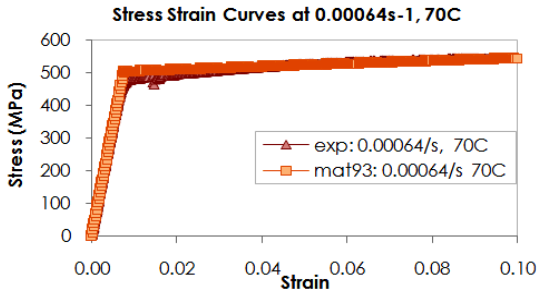

Fig. 16: Stress strain curves comparison between Mat93 and experimental data at $6.4\times10^{-4}sec^{-1}$, 70°C

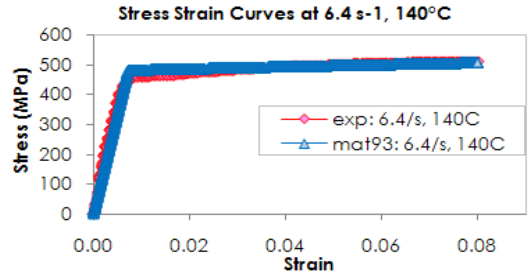

Fig. 17: Stress strain curves comparison between Mat93 and experimental data at 6.4×10^{-0} sec^{-1}, 140°C

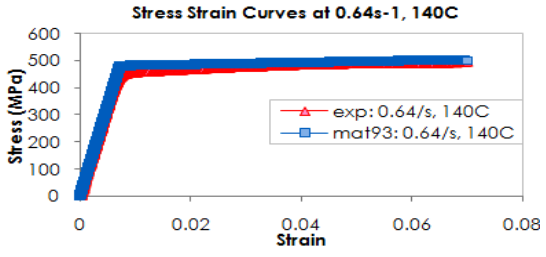

Fig. 18: Stress strain curves comparison between Mat93 and experimental data at 6.4×10^{-1} sec^{-1}, 140°C

and allow the plastic flow stress response (controlled by MTS model) of the constitutive model to be investigated.

Referring these figures, it can be observed that the proposed constitutive model shows a good agreement with the rate and temperature sensitivity of the specimen using the proposed approach. The flow stress that formulated as a function of the microstructural state has captured a reasonable relationship between stress, strain rate and temperature of Aluminium 7010. Very small variances between the simulation and the experimental results might be caused by the MTS properties used to control the flow stress of the new constitutive model.

Generally, it can be concluded that increasing strain rate increases the flow stress while increasing temperature decreases the flow stress. In other words, the saturation stress of the new material model increases with increasing strain rate and decreases with increasing temperature. Eventually, it is important to deduce that the analysis for the uniaxial tensile test for uniform plastic deformation of Aluminium 7010 can be validated using a single element, uniaxial stress test.

Up to this stage, the proposed approach to validate constitutive formulation of orthotropic materials and the corresponding algorithm is completely established. This particular model then can be further validated against the other related experimental tests. As can be found by (Mohd *et al*., 2013; Mohd, 2016) without any further modification, the model was successfully validated against a Plate Impact and Taylor Cylinder Impact tests to capture shockwave propagation and three dimensional stress state descriptions of the chosen orthotropic materials, respectively.

CONCLUSION

This study presents a simplified approach to validate constitutive model of orthotropic materials undergoing finite strain deformation. This approach is beneficial to systematically validate each part of the constitutive formulation and its algorithm implementation as the programming process is a cumbersome task. The validation process of related constitutive model can be considered completed at the end of the proposed validation process. Based on the results, it can be concluded that the formulation of the new constitutive model and its implementation was correct, hence validated. The yield points of each analysis were correctly determined. The elastic curves for both isotropic and orthotropic cases were correctly calculated based on the generated slopes.

The implementation of the Hill's yield criterion was also validated as the results were reasonably good when the analysis was set to isotropic case. The proposed approach also capables to investigate the hardening algorithm within the plasticity part to capture the new yield surface expansion in the new deviatoric plane. The

proposed method can demonstrates the MTS flow stress that agreed well with the tensile test data performed at various strain rates and temperatures.

At the end of this approach the proposed formulation can be further validated against related experimental data. For the chosen constitutive formulation adopted in this study, the model was then compared with respect to a Plate Impact and Taylor Cylinder Impact tests.

ACKNOWLEDGEMENTS

Researcher wishes to convey a sincere gratitude to Universiti Tun Hussein Onn Malaysia (UTHM) and Ministry of Higher Education Malaysia for providing the financial means during the preparation to complete this work under Fundamental Research Grant Scheme (FRGS), Vot 1547.

REFERENCES

Lin, J.I., 2004. DYNA3D: A nonlinear, explicit three-dimensional finite element code for solid and structural mechanics user manual. Lawrence Livermore National Laboratory, Livermore, California.

Mohd, N.M.K., 2012. Modelling rate dependent behaviour of orthotropic metals. Ph.D Thesis, Cranfield University, Cranfield, England.

Mohd, N.M.K., 2016. Modeling of constitutive model to predict the deformation behaviour of commercial Aluminum Alloy AA7010 subjected to high velocity impact. Modeling of constitutive model to predict the deformation behaviour of commercial Aluminum Alloy AA7 11: 2349-2353.

Mohd, N.M.K., R. Vignjevic and J. Campbell, 2013. Modelling shockwave propagation in orthotropic materials. Modelling shockwave propagation in orthotropic materials. 315: 557-561.

Panov, V., 2006. Modelling of behaviour of metals at high strain rates. PhD Thesis, Cranfield University, Cranfield, England.

Thomas, M.A., D.E. Chitty, M.L. Gildea and T.C.M. Kindt, 2008. Constitutive soil properties for cuddeback. MSc Thesis, Applied Research Associates Inc., Albuquerque, New Mexico. https://ntrs.nasa.gov/search.jsp?R=20080032551.